IET Microwaves, Antennas & Propagation

Research Article

IET Journals
The Institution of Engineering and Technology

Energy saving glazing with a wide band-pass FSS allowing mobile communication: up-scaling and characterisation

ISSN 1751-8725
Received on 17th August 2016
Revised 17th March 2017
Accepted on 11th May 2017
E-First on 17th July 2017
doi: 10.1049/iet-map.2016.0685
www.ietdl.org

Luc Burnier[1] ✉, Matteo Lanini[2], Olivia Bouvard[1], Damiano Scanferla[3], Abiraam Varathan[3], Carine Genoud[3], Arnaud Marguerit[4], Bernard Cuttat[4], Noémie Dury[5], Reiner Witte[5], Andrea Salvadè[2], Andreas Schüler[1]

[1]*Solar Energy and Building Physics Laboratory, Ecole Polytechnique Fédérale de Lausanne, Lausanne, Switzerland*
[2]*Telecom Telemetry High Frequency Lab, Dipartimento Tecnologie Innovative, University of Applied Sciences of Southern Switzerland, Galleria 2, CH-6928 Manno, Switzerland*
[3]*Innovation Department, Swisscom AG, P.O. Box, CH-3050, Bern, Switzerland*
[4]*AGC Verres Industriels SA, Quartier Verreries 25, CH-2740 Moutier, Switzerland*
[5]*Class 4 Laser Professionals AG, Industriering 43, Industriering 43, CH-3250 Lyss, Switzerland*
✉ *E-mail: luc.burnier@epfl.ch*

Abstract: A real case study and characterisation of modern energy efficient windows allowing mobile communication is presented. An earlier study had shown that laser scribing of energy saving coatings allows highly reducing the microwave attenuation (from 30 to 1–3 dB) using a wide band-pass frequency-selective surface (FSS) while preserving the thermal quality of the window. To achieve large-scale production, the laser scribing technique has been further developed. The effect of laser scribing on the mechanical properties of a substrate has been determined through mechanical strength tests. Moreover, the insulating properties of the window have been analysed to ensure the reliability of this technology. As a real case demonstration, an entire train has been equipped with prototype windows. The signal quality has been controlled for a wide band of frequencies and for existing technologies such as long term evolution, universal mobile telecommunication system, multiple input multiple output and for different configurations such as a stationary and a moving train.

1 Introduction

Modern energy saving windows are now commonly used in buildings and increasingly used in the transportation domain. They allow better insulation, which is necessary to meet current regulations of energy performance. Most are composed of a double glazing with a gap filled with different types of gas and a coating covering the inner side of one or both glass panes. The multilayer coating is made of a stack of oxide and metal thin films. It allows a high transmittance for visible light and a high reflectivity for higher wavelengths (middle and near infrared radiation). The metal layers also induce a high attenuation (around 33 dB) [1] of the telecommunication frequencies (TF) between 0.8 to 2.7 GHz. To overcome this unwanted effect, repeaters are increasingly used to obtain a good signal quality inside new buildings or trains. These systems are expensive, energy consuming and technologically dependent. Due to the rapid evolution of communication technology they need to be replaced every 5 to 8 years [2].

A frequency-selective surface (FSS) is a thin and repetitive surface designed to reflect, transmit or absorb electromagnetic fields [3]. FSS are mostly designed with a dimension according to the wavelength size [4, 5]. Earlier examples have been realised using etching or milling and by removing a significant percentage of the coated surface (5–15%). These FSS reduce the attenuation of a double glazing by 10 to 20 dB in the TF domain [6–9].

Our group has designed a FSS able to reduce the attenuation by 29 dB [10]. To obtain this filter, a grid is scribed in the layer by laser with a dimension smaller than the wavelength. We have shown that a grid of 2×2 mm^2 is a good compromise between ablated surface and microwave transmittance. This technique minimises the ablated area to a small percentage (<5%) and consequently preserves the thermal quality of the glazing.

In this study, the aim is to produce and characterise large-scale prototypes. The influence of different geometrical parameters of the glazing is examined using simulation. Moreover, thermal and mechanical properties are measured to ensure a reliable product. An entire train was equipped with prototype glazing, which allows for a real case study. The signal is characterised for a wide band of frequency and for existing networks.

2 Simulation

2.1 Theoretical approach

The proposed FSS design, realised with a $L \times L$ mm^2 square patch grating ($L = 2$ mm in this study), is considered as a non-resonant structure with capacitive behaviour. To analyse the frequency response of the FSS the analytical averaged approach described by Costa *et al.* [11] is used. The spacing and line width presented are at least five times smaller than [11] and the complete insulated glass unit (IGU) is modelled using electric circuit equivalence. The IGU used for this study is composed of a 5 mm grey glass pane, a 12 mm gap of dried air and a 4 mm float glass pane with coating. A series of transmission lines ($TRL_{1,2,3}$) simulate the propagation across the glass/air/glass dielectric slabs of the IGU (Fig. 1*a*); the resistor (R_{coat}) simulates the conductive coating (Fig. 1*b*) of standard IGUs, and a capacitor (C_{fss}) in series with a resistor (R_{fss}) is used for the FSS slab (Fig. 1*c*). The new structured IGU equivalent circuit is shown in (Fig. 1*d*).

The glazing was simulated using the following properties [6]: $\varepsilon_r = 7.0$, $\tan\delta = 0.001$; coating sheet resistivity: 4.0 Ω/sq.

At normal incidence, C_{fss} and R_{fss}, are calculated as follows [11, Eq. 2] [12, Eq. 8]:

$$C_{fss} = \frac{D\varepsilon_0(\varepsilon_{r1} + \varepsilon_{r2})}{\pi} \ln\left(\frac{1}{\sin(\pi w/2D)}\right) \quad (1)$$

$$R_{fss} \simeq R_{coating} \frac{D^2}{(D-w)^2} \quad (2)$$

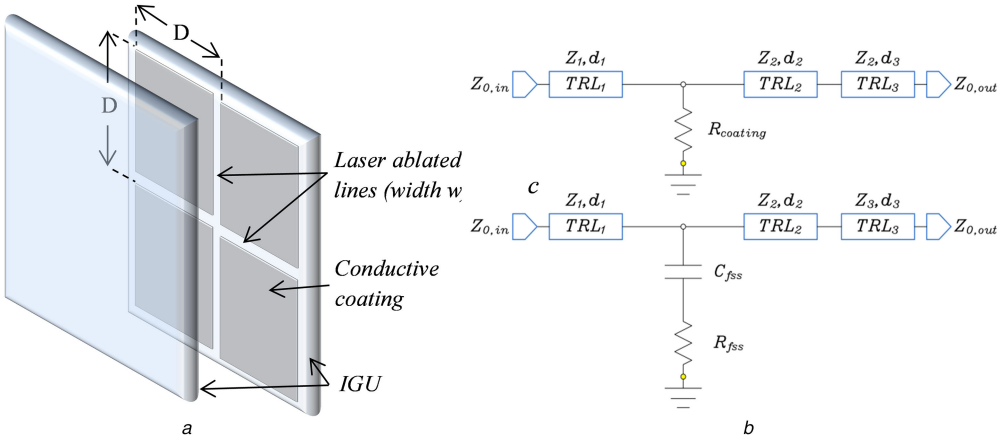

Fig. 1 *Series of transmission lines ($TRL_{1,2,3}$) simulate the propagation across the glass/air/glass dielectric slabs of the IGU, the resistor (R_{coat}) simulates the conductive coating, of standard IGUs, and a capacitor (C_{fss}) in series with a resistor (R_{fss}) is used for the FSS slab and the new structured IGU equivalent circuit*

(a) Schematic drawing of the IGU with a structured coating within a periodicity D delimited by the laser ablated lines, ***(b)*** Equivalent circuits of coated IGU with electrically conductive coating, ***(c)*** of IGU with new structured coating ($D \times D$ repetitive shapes)

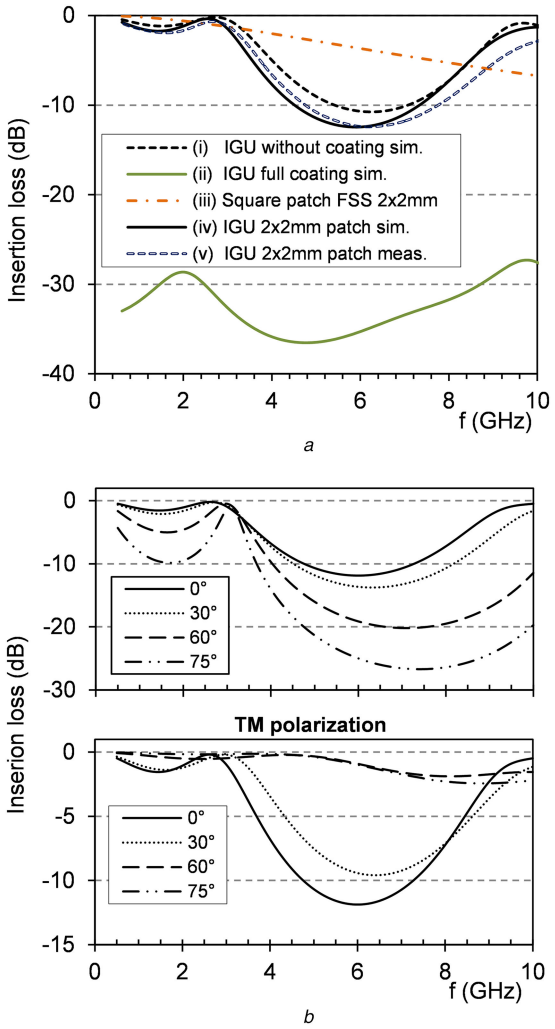

Fig. 2 *Insertion loss in the domain 0.5 to 10 GHz*

(a) Of the equivalent circuit models and a measurement (v) for comparison, ***(b)*** Of a IGU with the 2×2 mm^2 patch depending on the angle of incidence for TE and TM Polarisation

where $D = 2$ mm is the periodicity of the FSS; $w = 25$ µm is the width of the scribed lines; $R_{\text{coating}} = 4.1\ \Omega$ and ε_{r1}, ε_{r2} are the relative dielectric permittivity of the surrounding mediums (i.e. air and glass). Considering this parameters and (1) and (2) the calculated value are $R_{\text{fss}} = 4.1\ \Omega$ and $C_{\text{fss}} = 177.2$ fF.

For the TRL models, the impedance (Z_i) formula for ith dielectric slab is applied:

$$Z_i = \sqrt{\frac{\mu_0}{\varepsilon_0 \varepsilon_{\text{r},i}}} \tag{3}$$

where $\varepsilon_{r,i}$ is the relative dielectric permittivity of the ith slab (i.e. glass or air).

The impedance of the input and output ports of the circuit ($Z_{0,\text{in}}$, $Z_{0,\text{out}}$) and of the air gap Z_2 correspond to the free space wave impedance of $Z_0 = 376.7\ \Omega$. The impedance value of the glass panes are Z_1, $Z_3 = 142.4\ \Omega$.

To be able to simulate angular dependence the software ANSYS® HFSS™ (FEM) was used.

Fig. 2*a*, shows the results for different double glazing (IGU). The model allows obtaining the insertion loss due to the coating made of a square grid of 2×2 mm^2 SG2 (iii). The curve (iv) shows the results for a double glazing with a scribed coating 2×2 mm^2 (SG2) and (v) the measured value for comparison. Regarding Fig. 2*b*, the attenuation in the domain 0.5 to 3.5 GHz remains under 10 dB even for large angles of incidence. For the TM polarisation the attenuation is reduced for wide angles respecting the Brewster's law.

The results show a low attenuation in the RF used nowadays even for large angles of incidence. Moreover, the maximum attenuation is reached at a frequency of 6 GHz. This maximum is due to the structure of the IGU itself (total thickness) and slightly accented by the patterned coating (1–2 dB).

2.2 Parametric analysis

A parametric analysis was performed on the most relevant variations due to mechanical tolerances of the engraving and the glazing assembly.

The glazing tolerances, reported in Table 1 were chosen according to Tolerance Handbook [13]. An important parameter is the curvature of the glass, also known as 'general bow' (up to 2 mm/m) most of the samples presented a concavity >1 mm. To compare the theoretical results with the measurement of the prototypes, an average air-gap of 10 mm was chosen. The results are presented in Table 1.

The parametric analysis demonstrates that a variation of the line width of ±20% leads to a variation of attenuation under 2%. Moreover, for a standard variation of glass pane thickness the attenuation response remained almost unchanged. The air-gap variation shows a significant impact on the cut-off frequency shift and leads to a frequency downshift of about 8%. However, the cut-

Table 1 Parametric analysis of a double glazing regarding the cut of frequency (−3 dB) attenuation response

Parameter	Tolerance	Nominal	Minimum variation			Maximum variation		
	(±), mm	mm	dim., mm	f_{-3dB}, GHz	f_{-3dB}, %	dim., mm	f_{-3dB}, GHz	f_{-3dB}, %
glass thickness, slab 1	0.2	4	3.8	3.49	0.58	4.2	3.44	−0.86
glass thickness, slab 2	0.2	5	4.8	3.51	1.15	5.2	3.43	−1.15
air gap (bow of 2 mm)	2	10	8	3.81	9.8	12	3.2	−7.78
laser scribing width	0.005	0.025	0.02	3.44	−0.86	0.03	3.49	0.58

a *b*

Fig. 3 *To produce real size windows a computer numerical control CNC table with a large working dimension of 2.5 × 3 m² was equipped with a laser engraving system (Nd YAG laser) and a series of 34 windows of 1 × 1.4 m² was produced*

(a) Photograph of CNC allowing two directions motion (*XY*) with an acceptable dimension of 2.5 × 3 m² installed in an air filtered room AGC – VIM, ***(b)*** Photograph of the 34 train windows with scribed grid of 2 × 2 mm²

Table 2 *U* value for three types of glazing

U (W/m².K)±0.04		
Double glazing without coating	Double glazing with full coating	Double glazing scribed coating
2.89	1.86	1.87

off frequency remains highly above the frequencies used for mobile communication.

3 Up-scaling of the process

To produce real size windows a computer numerical control (CNC) table with a large working dimension of 2.5 × 3 m² (Fig. 3*a*) was equipped with a laser engraving system (Nd YAG laser). The system was installed in an air filtered room to reduce scribing defects due to the deposition of small particles on the surface.

The scribing was made from the non-coated side of the glass to achieve a clean film removal and this procedure is known to be more efficient compared with an irradiation from the coated side [14, 15]. An autofocusing system allows a positioning of the focal point on the coating with a high accuracy. The width of the scribed lines is maintained under 30 µm which allows making them almost invisible in normal conditions.

A series of 34 windows of 1 × 1.4 m² was produced (Fig. 3*b*). With respect to Fig. 2, a 2 × 2 mm² rectangular grid was chosen due to its simple design and its broad-band transmission in the RF domain. These windows were produced for the retrofit of a RABe 525 NINA train of the Swiss railway company BLS.

4 Characterisation of glazing properties

4.1 Thermal properties

The *U* and the g factor were measured to ensure the low effect of the laser ablation on insulating properties. For a grid pattern of 2 × 2 mm² and a line width of 25 µm the percentage of removed area of coating is 2.5% of the overall surface.

The *U* value is the thermal transmittance, it represents the heat transfer through one square metre, divided by the difference of temperature across a structure. It was measured by the Fraunhofer Institute for Solar Energy Systems according to DIN EN 674:2011. The measurement was performed on 800 × 800 mm² samples to reduce possible edge effects (Table 2).

The g factor represents the amount of solar energy passing through a structure, it was obtained for different incident angles from 0° to 75° with respect to the standard AFNOR – NF EN 410 [16] and using the method developed by Reber *et al.* [17]. The measurement was performed on samples with a dimension of 1200 × 800 mm² to avoid edge effects. The samples were composed as presented before. The tested double glazing was filled with dried air to avoid possible errors due to the filling rate of special gases.

The double glazing without coating shows standard *U* and *g* values. The coating reduces the *U* value by a factor of 1.5. Regarding Table 2 and Fig. 4 the *U* and *g* value modifications remains below the measurement error (<2 and <5%, respectively, for considering the uncertainty). The performed measurements prove the small impact of the laser scribing on the thermal quality of the window.

4.2 Mechanical properties

For safety rules the glass can be tempered. This process creates mechanical stresses in the glass and so causes the glass to crumble when it is broken. To ensure a high-mechanical resistance of the modified glass pane a coaxial double ring test setup was used and the calculation respected the Roark formula.

For each type of sample, a series of at least six samples was prepared to obtain statistically reliable data. Tempered glass with full coating served as reference. The maximum constraints before the fracture of the glass with its standard deviation are presented in Table 3.

From Table 3, the mechanical properties of the glass pane scribed before tempering are not modified. The deviation compared with a non-treated glass is below the error of measurement.

For the sample scribed after the tempering, our measurement suggests that the laser ablation might have an influence on the

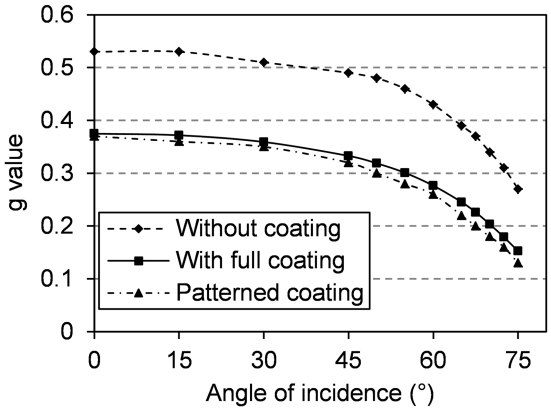

Fig. 4 *g factor depending on the angle of incidence and of the type of glazing*

Table 3 Constraint results and standard deviation

	Number of samples	Constrain max, Mpa	
		Average	Std. dev.
tempered glass full coating	6	450.1	91.2
laser scribed then tempered	10	484.6	60.8
tempered then laser scribed	17	391.6	16.9

mechanical properties of the substrate. The maximum constraint is reduced by a relative 13% compared with a glass with full coating.

It has been shown that laser scribing leaves a heat affected area, where the temperature can reach the order of magnitude of 1200 K [18] around the scribed point. It might modify the mechanical properties of tempered glass. To preserve the mechanical properties of the glass it might be preferable to scribe the coating before the tempering process. Moreover, the attenuation has been measured before and after the tempering and does not present significant changes.

4.3 Quality control of produced train windows

The insertion loss of each window was measured ranging from 0.85 to 5 GHz with a free-space measurement setup with a time-gate filter as described in [19–21]. As the measured sample is electrically large, the attenuation can straightforwardly be obtained from the difference between a reference measurement (antenna in unobstructed line of sight) and with the sample fixed on a simple holder.

Regarding the results given in Fig. 5, the standard deviation remains really small in the domain of 0.85 to 3.5 GHz. Furthermore, for higher frequencies (above cut-off frequency) the standard deviation increases slightly, this effect could be explained by the air-gap deviation.

5 Train with novel prototype glazing

For the train retrofit project prototyped windows were installed to avoid the installation of repeater. This train allows a real case scenario, the performance of existing telecommunication network have been tested.

5.1 Measurement of attenuation in a stationary train

A measurement campaign was carried out on two stationary trains, one equipped with standard non-coated windows and one equipped with the prototyped windows. The aim is to analyse the impact of the scribed coating compared with non-coated double glazing. Two measurements have been performed for each train, one on a wide band of frequencies and a second one, on existing mobile radio signals universal mobile telecommunication system (UMTS – at 900 and 2100 MHz, and LTE at 800 and 1800 MHz).

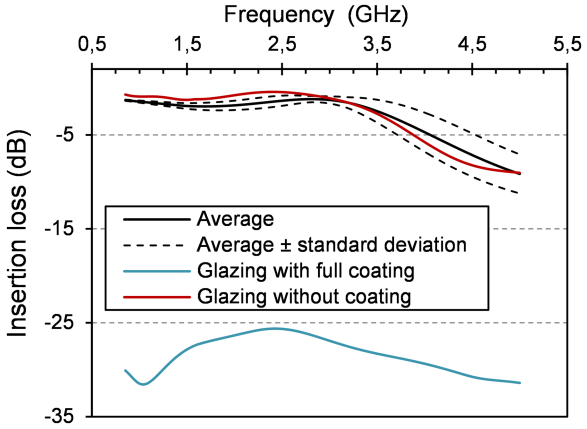

Fig. 5 *Insertion loss measurement of the series of windows (34 measurements) and its standard deviation in the frequency domain from 0.85 to 5 GHz*

The purpose of the wide band measurement was to evaluate the difference within the two trains over a frequency range comparable with laboratory measurements as well as to analyse the effect of the wave polarisation and include oblique polarisation (±45° pol.). One emitting antenna (EA – R&S HL050) was placed outside the train and a receiver antenna was placed in the carriage (Fig. 6*a*). A sweeping CW signal was generated by a signal generator (Agilent PSG E8257E) and acquired with a spectrum analyser (Agilent PSA E4446A). Both were synchronised to avoid transmissions on busy channels, thus minimising external interferences. The EA was moved along the carriage to take into account oblique angles of incidence and different polarisations (± 45° and vertical).

The insertion loss is measured for both trains and calculated as the average signal for each EA position and for the different polarisations. In Fig. 7*a*, the attenuation presented is the difference between the average signal of the train with standard glazing and the train with novel glazing.

The purpose of the second measurement is to compare the outdoor (close to the carriage) to indoor (corridor and seats area) attenuations of UMTS and LTE signals between the two trains. The attenuation was calculated as the difference between the medians of the signal strength distributions for each antenna (Fig. 6*b*), The measurements were carried out with a dipole antenna (Kathrein 80010847) connected to the radio network analyser R&S TSMW and collected with a laptop running Nemo Outdoor [22]. The signal strength was obtained from the pilot signals of UMTS 900–2100 MHz and LTE 800–1800 MHz which are independent from the load of the network (Fig. 7*b*).

The two trains were measured sequentially and in the same location to ensure a similar angle of incidence. The attenuation measurements include the effects of the windows but also the train structure and the interior composition (the two trains were not perfectly identical, e.g. train compartment separated by walls). This fact may induce a positive or negative deviation on the results.

For both measurements (Figs. 7*a* and *b*) the difference of attenuation between the two trains remains in almost all cases below the uncertainty of ±2 dB.

5.2 Measurement in a moving train

Another measurement campaign was carried out to compare the mobile network performance that a user would experience travelling inside a train with the prototyped glazing, compared with a train with standard non-coated glazing. The test train was composed of two coupled RABe 525 NINAs, each one with a different type of windows, and each one with 3 carriages. The measurement campaign consisted of six return journeys between Ostermundigen and Thun distributed over 2 days and focused on three technologies of the Swisscom mobile network that provided continuous coverage along the track: UMTS 900 MHz (5 MHz carrier), UMTS 2100 MHz (5 MHz carrier), and LTE 1800 MHz [20 MHz bandwidth and 2 × 2 multiple input multiple output (MIMO)].

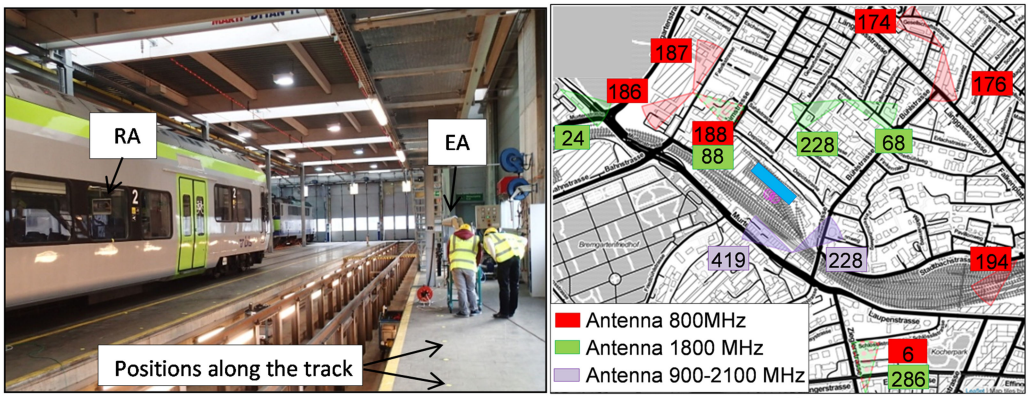

a b

Fig. 6 *One emitting antenna (EA – R&S HL050) was placed outside the train and a receiver antenna was placed in the carriage and the attenuation was calculated as the difference between the medians of the signal strength distributions for each antenna*

(a) Photography of the train in the workshop, ***(b)*** Map showing the train position (rectangle), the orientation of the antennas on site and their identification codes for the technologies LTE and UMTS

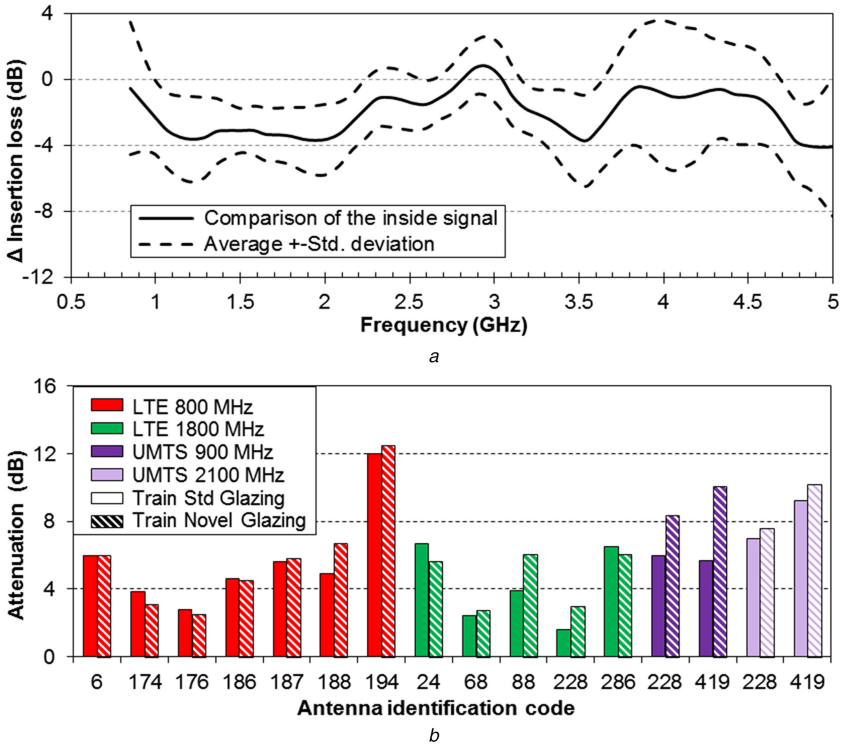

Fig. 7 *Comparison of attenuation signal between a train with novel glazing and one with standard glazing*

(a) Frequency dependent difference of the average attenuation for polarisation vertical and ±45°, ***(b)*** Evaluation of different technologies LTE, UMTS, the bars show the attenuation in signal level from the outside to the inside

For the pilot test, the aim was to compare the signal strength inside the two trains using calibrated equipment. The three technologies were measured simultaneously with the same equipment of the outdoor measurement described in 5.1.

For the downlink test two Samsung S5s were locked to UMTS-2100 MHz and LTE-1800 MHz both connected to a laptop running Nemo Outdoor and a Samsung Note 4 was locked to UMTS-900 MHz running Nemo Handy-A pro [22]. The downlink test consisted in an FTP download of either one file with five parallel threads or three files in parallel, depending on the device. Multiple files or threads are required to fully utilise the radio interface. The exact same test was repeated three times for each train in three different locations in the carriage. The train position in real time was obtained using a GPS antenna.

For a fair comparison of subsequent journeys, the track was sliced into segments of 25 m and only the average of the samples that fell in each segment was used to calculate the cumulative distribution function (CDF) of each quantity in every trip. Fig. 8 shows the CDF of the received signal code power (RSCP) and the downlink MAC throughput for UMTS 2100.

The results are very similar for both trains. The continuous line shows the results for the train with standard windows and the dotted line shows the results of the train with prototyped windows.

The results of the pilot test and of the downlink test are summarised, respectively, in Tables 4 and 5. Reference signal received power (RSRP) and reference signal signal-to-noise ratio (RSSNR) for LTE. Rank 2 utilisation is the percentage of time of the measurement samples in which spatial multiplexing (MIMO with two data streams) was used rather than transmit diversity (MIMO with one data stream). The 95th percentile (95%ile) column presents the value below which 95% of the samples fall.

The measurements show a slightly higher median signal attenuation for the prototyped glazing compared with standard glazing (0.1–1.8 dB). However, this result may be partially affected by the uncertainty of the measurement and by the differences in the interiors of the carriages. Furthermore, the downlink throughput for all three technologies is almost identical and the Rank 2 utilisation for LTE indicates very similar MIMO properties. These results are in agreement with those of the stationary measurement.

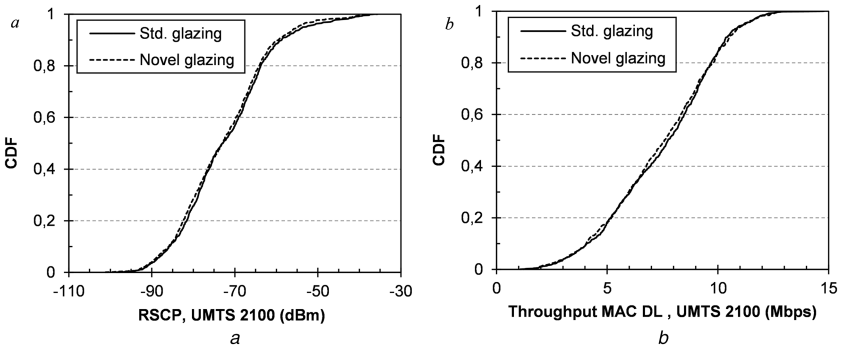

Fig. 8 *Distribution of the CDF value for the technologies UMTS 2100. as a function of*
(a) Insertion loss level and ***(b)*** Of the throughput for the train equipped with novel glazing and the one equipped with standard glazing

Table 4 Results of the pilot test, the reported values are in the form median / 95%ile

	Standard glazing		Prototyped glazing		S-P/S, %
	Median	95%	Median	95%	
LTE 1800 – RSRP, dBm	−86.2	−70.0	−87.5	−71.8	1.6
UMTS 900 – RSCP, dBm	−59.5	−43.7	−60.6	−44.8	1.8
UMTS 2100 – TSCP, dBm	−66.6	−52.5	−68.4	−53.2	2.7

Table 5 Results of the downlink test, the reported values are in the form median/95%

LTE-800	RSRP, dBm	−89.9	−73.9	−90.1	−74.8	0.3
	throughput, Mbps	51.2	102.3	50.4	102.5	−1.5
	RS SNR, dB	12.2	20.3	12.1	21.1	−1.3
	rank 2 utilization, %	85.7	98.6	83.1	98.5	−3.0
UMTS-900	RSCP, dBm	−65.8	−49.7	−67.3	−51.7	2.3
	throughput, Mbps	7.1	10.0	7.1	7.1	0.3
UMTS-2100	RSCP, dBm	−72.9	−53.5	−73.0	−54.8	0.2
	throughput, Mbps	7.4	10.7	7.2	10.7	−2.2

6 Discussion

Owing to a wide band-pass the new window can pretend to a long lifetime (20 to 25 years) compared with repeaters which are technologically dependent (change every 5 to 8 years) and consume energy. Future technology might be oriented to higher frequencies which would need smaller distances between antennas and could be problematic for outdoor – indoor coverage [5]. However, the cut-off frequency could be adapted by reducing the cell size (e.g. 1×1 mm^2 grid) and the line width proportionally, to ensure minimal impact on the thermal properties of the window. Moreover, it has been shown that the laser scribing might modify the mechanical properties of tempered glass panes. To overcome this effect an additional study has to be run to reduce the impact on the tempered glass substrate by optimising the laser parameters. Already on prototype scale this solution is financially competitive compared with repeaters. The novel glazing might also be interesting for building integration but a better understanding of wave penetration in large structures is needed [23].

7 Conclusion

A large-scale production of modern windows allowing mobile telecommunication was presented. Large-scale glazing with a wide band-pass FSS of commercial low-emissivity coatings has been produced by laser processing. Thermal properties (U, g) have been measured and show almost no deviation compared with a fully coated glazing. Moreover, the effect of laser ablation is avoided by tempering the glass after the laser scribing process. A quality control has shown a small variation of attenuation for a large number of windows and the attenuation remained under 3 dB in the telecommunication frequency domain (improvement of 27 dB compared with coated glazing). Using simulation the gap between the two glass panes has shown the highest influence on the attenuation response. An entire train has been equipped with prototype windows and tested in real conditions. This study shows a high-signal transmission in the prototype window equipped train compared with one with standard windows (<1.8 dB). The measurements of attenuation for the wide band-pass and for current technology (LTE and UMTS) are almost not affected by the scribed coating. The presented glazing with a wide band-pass FSS made by laser scribing can be a promising alternative to commonly used signal amplifier.

8 Acknowledgment

We express our utmost gratitude towards the Swiss Federal Office of Transport that made this research possible. We are also thankful to our industry partners, especially to Mr Maushart, AGC-VIM and to C. Isenschmid from the railway company BLS for their general support. We also thank P. Loesch for technical support, to P. Oelhafen for the inspiration and discussion, and to S. Taylor for the proof reading.

9 References

[1] Kiani, G.I., Olsson, L.G., Karlsson, A., *et al.*: 'Transmission of infrared and visible wavelengths trough energy-saving glass due to etching of frequency-selective surfaces', *IET Microw. Antennas Propag.*, 2010, **4**, (7), pp. 955–961
[2] Panwar, N., Sharma, S., Singh, A.K.: 'A survey on 5G: the next generation of mobile communication', *Phys. Commun.*, 2016, **18**, pp. 64–84
[3] Munk, B.A.: '*Frequency selective surfaces, theory and design*' (2005)
[4] Kiani, G.I., Aldhaheri, R.W.: 'Wide band FSS for increased thermal and communication efficiency in smart buildings'. IEEE Antennas and Propagation Society Int. Symp. 2014, 2014
[5] Asp, A., Baniya, A., Yunas, S.F., *et al.*: 'Applicability of frequency selective surfaces to enhance mobile network coverage in future energy-efficient built environments'. European Wireless, 2015
[6] Kiani, G.I., Karlsson, A., Olsson, l.: 'Glass characterization for designing frequency selective surfaces to improve transmission through energy saving glass windows'. CODEN: LUTEDX/(TEAT-7170)/1-7, 2008
[7] Gustafsson, M., Karlsson, A., Rebelo, A.P.P., *et al.*: 'Design of frequency selective windows for improved indoor outdoor communication'. CODEN: LUTEDX/(TEAT-7132)/1-14, 2005
[8] Sohail, S.I., Zarar, M.: 'Frequency selective surface for RF/microwave signal transmission in energy-saving glass', *ARPN J. Eng. Appl. Sci.*, 2015, **10**, (19)

[9] Kiani, G.I., Irfan, S.I., Esselle, K.P.: 'Design of a bandpass FSS on dual layer energy saving glass for improved RF communication in modern buildings'. IEEE 978-1-4673-0462-7/12, 2012
[10] Bouvard, O., Lanini, M., Burnier, L., *et al.*: 'Structured transparent conductive coatings with dual spectral selectivity across the terahertz region', *Appl. Phys. A*, 2017
[11] Costa, F., Monorchio, A., Manara, : 'An overview of equivalent circuit modeling techniques of frequency selective surfaces and metasurfaces', *ACES J.*, 2014, **29**, (12)
[12] Costa, F., Monorchio, A., Manara, G.: 'Analysis and design of ultra thin electromagnetic absorbers comprising resistively loaded high impedance surfaces', *IEEE Trans. Antennas Propag.*, 2010, **58**, (5), pp. 1551–1558
[13] Tolerance Handbook, Single Glazing and Insulating Glass Units, AGC Interpane. Available at http://www.interpane.com/medien/service2011/interpane_tolerance_handbook_01-2013en_rev-.pdf
[14] Witte, R., *et al.*: 'Investigation of a reliable all-laser scribing process in thin film Cu(In,Ga)(S,Se)$_2$ manufacturing'. Proc. SPIE 8607, Laser Applications in Microelectronic and Optoelectronic Manufacturing (LAMOM) XVIII, 86071B, 2013
[15] Beyer, S., Tornari, V., Gornicki, D.: 'Comparison of laser induced front- and rear side ablation'. Proc. of SPIE, 2003, vol. **5063**
[16] NF EN 410, Glass in building, Determination of luminous and solar characteristics of glazing, AFNOR 2011
[17] Reber, G., *et al.*: 'Angular dependent solar gain for insulating glasses from experimental optical and thermal *data*'. Proc. of CISBAT, EPFL. 2005, 2005
[18] Wang, H., Hsu, S.T., Tan, H., *et al.*: 'Predictive modeling for glass-side laser scribing of thin film photovoltaic cells'. Proc. of NAMRI/SME, 2012, vol. **40**
[19] Wilson, P.F., Ma, M.T., Adams, J.W.: 'Techniques for measuring the electromagnetic shielding effectiveness of materials. I. Far-field source simulation', *IEEE Trans. Electromagn. Compat.*, 1988, **30**, (3), pp. 239–250
[20] Grosvenor, C.A., Novotny, D., Johnk, R., *et al.*: 'Shielding effectiveness measurements using the direct illumination technique'. IEEE Int. Symp. on Electromagnetic Compatibility, 2002. EMC 2002. 19–23 August 2002, vol. **1**, pp. 389–394
[21] Agilent 'Time Domain Analysis Using a Network Analyzer', Application Note 1287-12
[22] http://www.anite.com/businesses/network-testing
[23] 'Technical feasibility of IMT in bands above 6 GHz'. Report ITU-R M. 2376-0(07/2015)